

## CHAPTER VI CHANGES OF MIDGAP STATES

annealed at 150 and 200 °C. The  $g(E)$  after light exposure increased by a factor of about 1.7 compared with the  $g(E)$  for the as-deposited film, but the energy position of the peak of midgap states did not change by light exposure. After annealing at 150 °C for 3 h, the  $g(E)$  for  $(E_C-E)$  in the range higher than 0.8 eV decreased. In the film annealed at 200 °C for 1.5 h, the  $g(E)$  for  $(E_C-E)$  in the range higher than 0.85 eV approached to the  $g(E)$  for the as-deposited film, while for  $(E_C-E)$  in the range lower than 0.85 eV it was still larger than the  $g(E)$  for the as-deposited film. The value of  $E_a$  which was roughly estimated from this experiment is shown in Fig. 6.8(b), and  $E_a$  seems to get saturated in lower  $(E_C-E)$ .

This is the first report which elucidates the relation between  $E_a$  and  $(E_C-E)$ . Although Stutzmann et al.<sup>4)</sup> and Smith et al.<sup>6)</sup> predicted that midgap states should have a distribution of  $E_a$ , they did not discuss the relation between  $E_a$  and  $(E_C-E)$ . The values of  $E_a$  are similar to those reported by Qiu et al.,<sup>8)</sup> while they are rather larger than those reported by Stutzmann et al..<sup>4)</sup> Shepard et al.<sup>13)</sup> have predicted from photoconductivity measurements that the  $g(E)$  above the Fermi level (maybe doubly-occupied dangling bonds,  $D^-$ ) closest to the midgap is annealing first, with which the present results coincide if the correlation energies between  $D^0$  and  $D^-$  are kept constant.

### 6-4. Optically and Thermally Induced Reversible Changes of Midgap States in Undoped a-Si:H

Undoped a-Si:H/p c-Si heterojunctions were fabricated as follows. Undoped a-Si:H films (1.2-1.5  $\mu\text{m}$  thickness) were deposited by the rf glow-discharge decomposition of pure  $\text{SiH}_4$  gas onto p c-Si substrates heated to  $T_s=200-300$  °C. After turning off the plasma, the substrate temperature was kept as it was for 10 min. Then the specimen was cooling down slowly. The acceptor density ( $N_A$ ) in p c-Si was  $1.0 \times 10^{16} \text{ cm}^{-3}$ . Since Mg is known to form a good Ohmic contact with undoped a-Si:H, Mg was evaporated on an area ( $0.785 \text{ mm}^2$ ) of as-deposited films at room temperature

## CHAPTER VI CHANGES OF MIDGAP STATES

(as-deposited films). For other heterojunctions, Mg was evaporated at room temperature after the a-Si:H films were exposed to AM1 light with  $100 \text{ mW/cm}^2$  at room temperature (light-soaked films), or after those films, which had been kept at a given high temperature ( $T_{RC}$ ) in  $H_2$  atmosphere for 10 min, were immediately dropped into liquid nitrogen (rapidly-cooled films).

The midgap-states density ( $N_I$ ) of undoped a-Si:H was estimated from the high-frequency (1-MHz) capacitance-voltage (C-V) characteristics at room temperature using the steady-state HMC method, as mentioned in Chapter III. The HMC signals of  $H(t)$ , which are obtained from the transient capacitances of their heterojunctions measured at 2 MHz, approximately correspond to their density-of-states distributions  $[g(E)]$  through (See Chapter IV)

$$g(E) = H(t)/kT \quad , \quad (6-8)$$

and the energy location below the conduction band edge ( $E_C$ ) is expressed by

$$E_C - E = kT \ln(\nu_n t) \quad , \quad (6-9)$$

where  $k$  is the Boltzmann's constant,  $T$  is the measuring absolute temperature,  $t$  is the time after the reverse bias is applied to the junction,  $\nu_n$  is the attempt-to-escape frequency for electrons which can be estimated from the temperature dependence (353-393 K) of the time ( $t_p$ ) at the peak of  $H(t)$ .

First, the illumination-time dependence is considered. The value of  $N_I$  increased with about one-third powers of the illumination time ( $t_{IL}$ ), whose behavior was quite similar to the results obtained from the ESR measurements, as described in Section 6-1. The value of the activation energy ( $\delta_2$ ) of dark conductivity of the film was independent of  $t_{IL}$  as long as  $t_{IL}$  was longer than 3 h. The value of  $\delta_2$  of light-soaked films, however, was larger than that of as-deposited films, as is similar to the data in Table 6-1. The  $H(t)$  signals did not change before and after the as-deposited film was annealed at 200

## CHAPTER VI CHANGES OF MIDGAP STATES

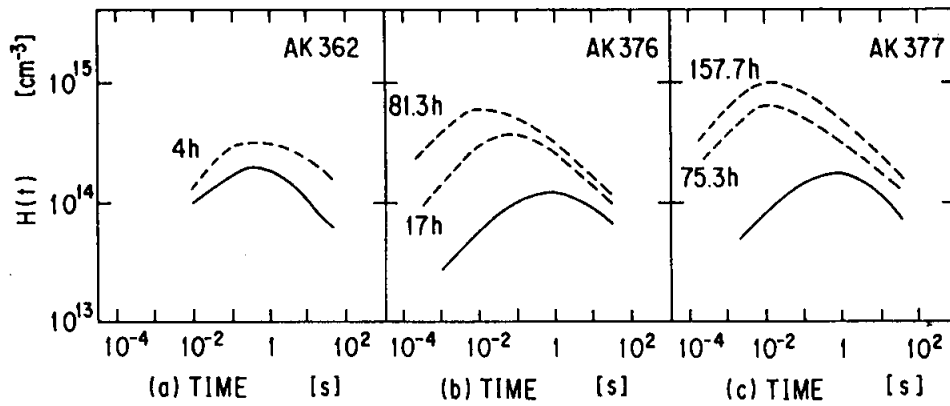


**Fig.6.9.** Dependence of  $H(t)$  signals on illumination time: (a) 4-h illumination on sample AK362; (b) 17 h and 81.3 h on AK376; and (c) 75.3 h and 157.7 h on AK377. The solid curves represent  $H(t)$  for as-deposited films.

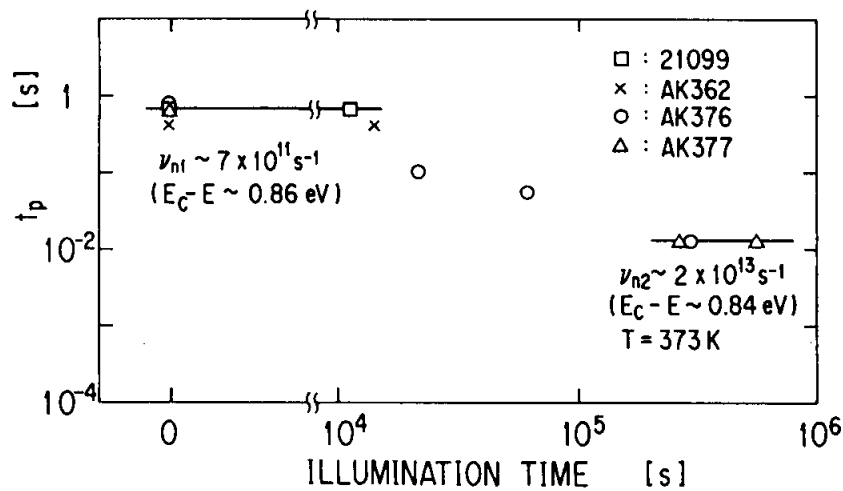


**Fig.6.10.** Dependence of time( $t_p$ ) on illumination time( $t_{IL}$ ). The solid lines are guides to eye.

## CHAPTER VI CHANGES OF MIDGAP STATES

°C for 2 h in a vacuum, and the  $H(t)$  signals for the films annealed at 200 °C for 2 h after the light soaking were quite similar to those for as-deposited films.

Figure 6.9 shows the dependence of  $H(t)$  signals on  $t_{IL}$ . After short-time ( $\leq 4$ -h) light soaking, the magnitude of  $H(t)$  increased without any shift of  $t_p$ , while after long-time ( $\geq 75$ -h) light soaking  $t_p$  was shifted toward shorter time and kept constant, as is clearly shown in Fig. 6.10. From the temperature dependence of  $t_p$ ,  $\nu_n$  and the energy position ( $E_C - E_p$ ) corresponding to the peak of  $H(t)$  were estimated;  $\nu_{n1}$  and ( $E_C - E_{p1}$ ) for the as-deposited and the short-time light-soaked films were about  $7 \times 10^{11} \text{ s}^{-1}$  and 0.86 eV, respectively, and  $\nu_{n2}$  and ( $E_C - E_{p2}$ ) for the long-time light-soaked films were about  $2 \times 10^{13} \text{ s}^{-1}$  and 0.84 eV, respectively. Although the change of  $t_p$  could, as one possibility, be thought to arise from the change of the free electron concentration in the depletion region of a-Si:H which leads to the change in the reverse current of the heterojunction,<sup>14)</sup> the reverse current for the long-time light-soaked film was the same as that for the as-deposited film, indicating that the change of  $t_p$  must originate from the change of  $\nu_n$ . Figure 6.11 schematically summarizes the above results. The solid curve A represents the  $g(E)$  in the as-deposited film. After the short-time light-soaking, both midgap states increased. However, the midgap states with  $\nu_{n2}$  (the dashed curve B1) are still hidden by those with  $\nu_{n1}$  (the solid curve B1). Subsequent light-soaking makes the midgap states with  $\nu_{n2}$  (the dashed curve B2) larger than those with  $\nu_{n1}$  (the solid curve B2). Therefore, the rate of increase of midgap states with  $\nu_{n2}$  must be larger than that with  $\nu_{n1}$ .

Second, the change of light-soaked films by thermal annealing is discussed. Figure 6.12(a) shows the changes of  $H(t)$  for the long-time light-soaked films by a 150-°C annealing for 2 h, and Fig. 6.12(b) shows those by a 200-°C annealing. Since the  $H(t)$  signals include information on two kinds of midgap states, two sorts of energy scales corresponding to  $\nu_{n1}$  and  $\nu_{n2}$  are shown in the abscissa below the time scale. Section 6-3 has studied the thermal annealing kinetics using the short-time

# CHAPTER VI CHANGES OF MIDGAP STATES

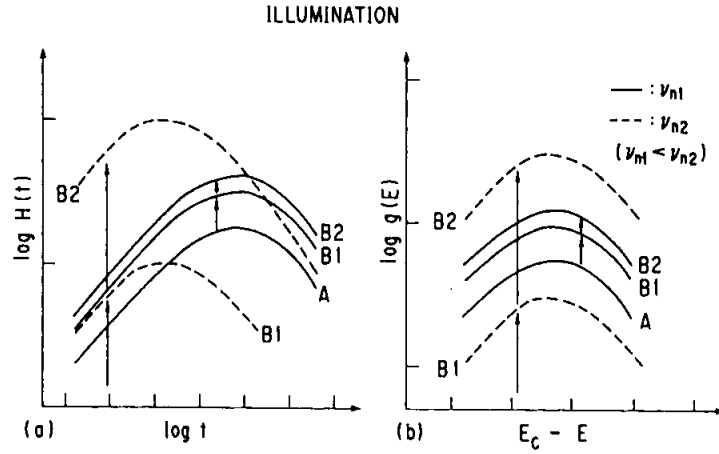


**Fig.6.11.** Schematic changes of midgap states by light soaking. The solid and dashed lines represent the states with small and large  $\nu_n$ , respectively. A, B1, and B2 correspond to the as-deposited (or completely annealed), the short-time light-soaked, and the long-time light-soaked films, respectively. (b) is estimated from (a) using the relations of  $g(E)=H(t)/kT$  and  $E_c-E=kT\ln(\nu_n t)$ .

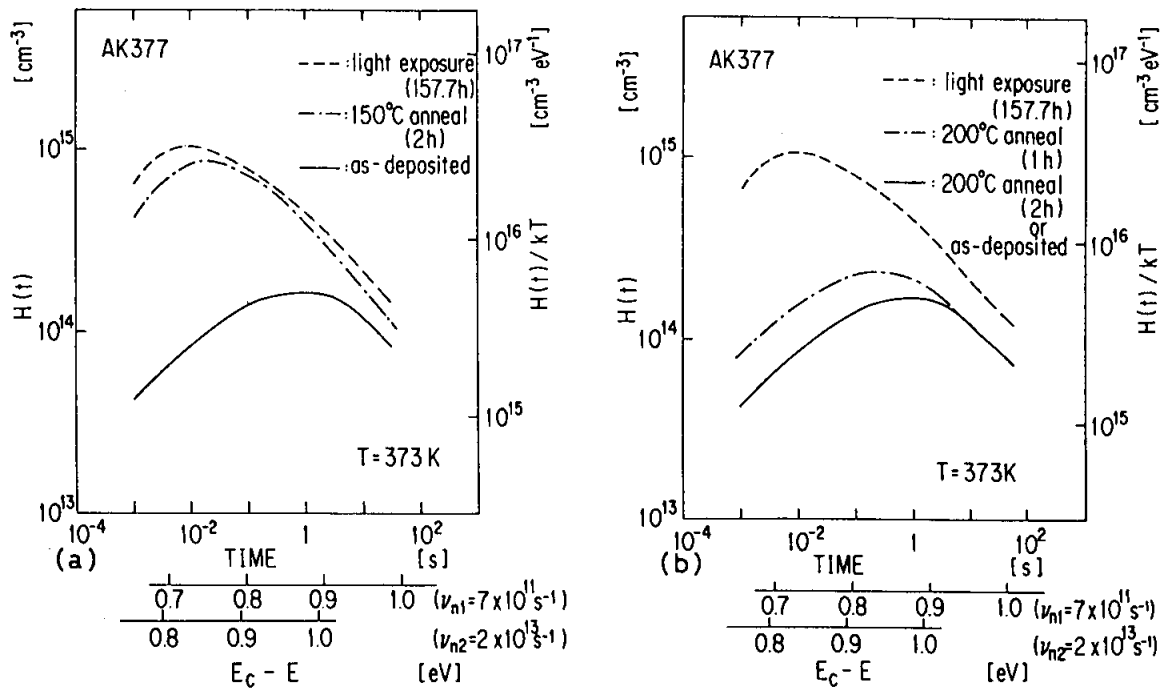


**Fig.6.12.** Changes of measured  $H(t)$  by (a) 150-°C annealing and (b) 200-°C annealing for long-time light-soaked film.

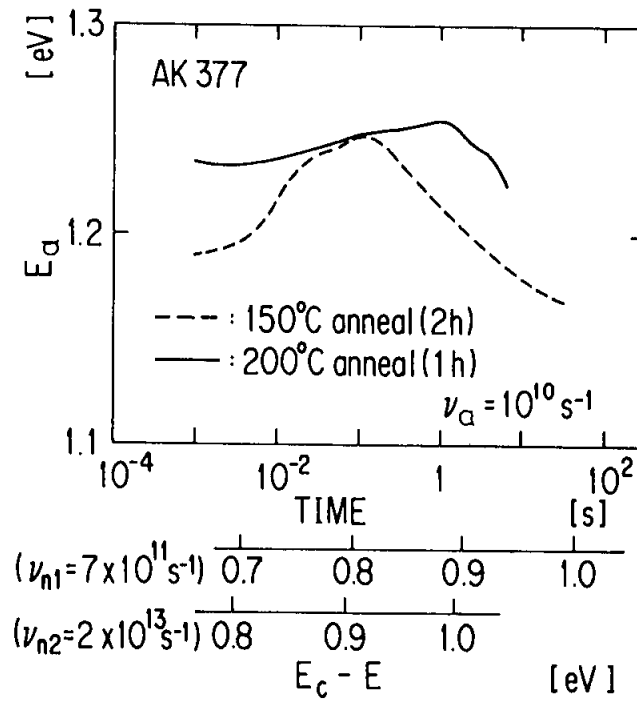


**Fig.6.13.** Activation energies estimated from studies of annealing at 150 °C for 2 h and subsequent annealing at 200 °C for 1 h.

## CHAPTER VI CHANGES OF MIDGAP STATES

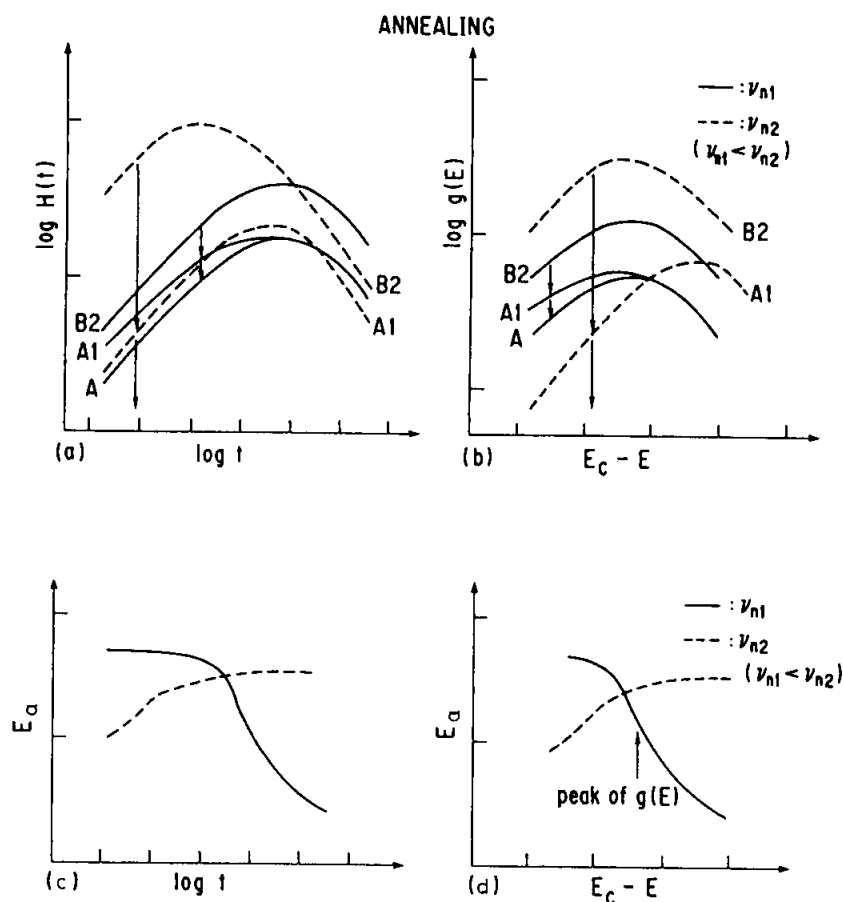


**Fig.6.14.** Schematic changes [(a) and (b)] of midgap states by thermal annealing and activation energies [(c) and (d)] for thermal annealing. The relation between  $(E_C - E)$  and  $t$  is given by  $E_C - E = kT \ln(\nu_n t)$ . The relation between  $H(t)$  and  $g(E)$  is expressed as  $g(E) = H(t)/kT$ . The solid and dashed lines represent the states with small and large  $\nu_n$ , respectively. B2, A1, and A correspond to the long-time light-soaked, the short-time annealed, and the completely annealed films, respectively.

## CHAPTER VI CHANGES OF MIDGAP STATES

light-soaked films, from which the monomolecular annealing kinetics are found to be suitable for explaining those results. Figure 6.13 shows the activation energies for the 150-°C annealing (2 h) and the 200-°C annealing (1 h) from Fig. 6.12, assuming a monomolecular annealing process. In Fig. 6.13, the dashed curve at  $t > 10^{-1}$  s and the solid curve at  $t < 10^{-1}$  s are quite similar to the curve shown in Fig. 6.8, and those curves represent the activation energies for midgap states with  $\nu_{n1}$ . So, the dashed curve at  $t < 10^{-1}$  s and the solid curve at  $t > 10^{-1}$  s must be affected by the activation energies for the midgap states with  $\nu_{n2}$ . Since the energy dependence of  $E_a$  for the short-time light-soaked films is already known as shown in Fig. 6.8, changes in  $E_a$  and  $H(t)$  for the annealing process in the long-time light-soaked films can be schematically described as shown in Fig. 6.14. After the long-time light-soaking, there are the midgap states with  $\nu_{n1}$  (the solid curve B2) and those with  $\nu_{n2}$  (the dashed curve B2). The annealing at 150 °C for 1 h makes the midgap states decrease a little. Those decreases of midgap states correspond to that of the midgap states with  $\nu_{n2}$  at  $t < 10^{-1}$  s and that of those with  $\nu_{n1}$  at  $t > 10^{-1}$  s. Midgap states with  $\nu_{n2}$  still dominate at  $t < 10^{-1}$  s and those states with  $\nu_{n1}$  are still dominant at  $t > 10^{-1}$  s. The annealing at 200 °C for 1 h makes the midgap states decrease to the curve of A1. The value of  $E_a$  at  $t < 10^{-1}$  s is close to that with  $\nu_{n1}$ , and  $E_a$  at  $10^{-1} \text{ s} < t < 1 \text{ s}$  must be close to that with  $\nu_{n2}$ . In final, the subsequent 200-°C annealing for more 1 h gets the midgap states with  $\nu_{n2}$  hidden by those with  $\nu_{n1}$  (the solid curve A).

Third, the effect of rapid cooling is mentioned using Fig. 6.15. Smith and Wagner<sup>6)</sup> have combined the creation process with the annealing process, where both have been proposed by Stutzmann et al.<sup>3,4)</sup>;

$$dN_s/dt = c_{sw}np - \nu_a \exp(-E_a/kT)N_s \quad (6-10)$$

and the product of  $n$  and  $p$  in the dark is expressed by

$$np = N_C N_V \exp(-E_{g2}/kT) \quad , \quad (6-11)$$



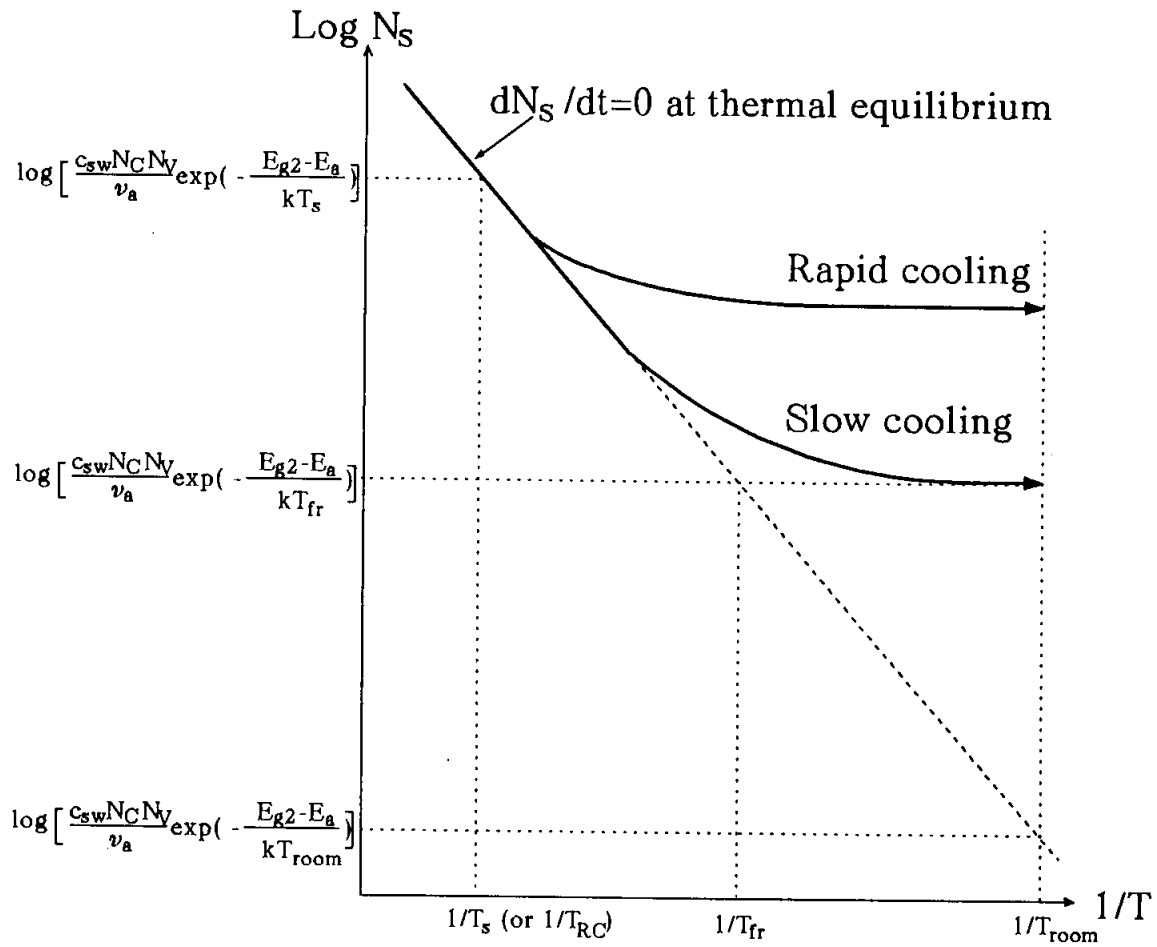


Fig.6.15. Schematic sketch of temperature-dependent midgap-state density.

## CHAPTER VI CHANGES OF MIDGAP STATES

where  $N_S$  is the total density of midgap states and  $c_{sw}$  is the constant related with the Staebler-Wronski effect,  $n$  and  $p$  are the free carrier densities in the conduction band and the valence band, respectively, and  $N_C$  and  $N_V$  are the effective densities of states in the conduction band and the valence band, respectively. During the deposition at a substrate temperature ( $T_S$ ) or keeping the film at a given temperature ( $T_{RC}$ ), the equilibrium condition ( $dN_S/dt=0$ ) is assumed to be held. In this case, the total density of midgap states is expressed as

$$N_S = (c_{sw}N_CN_V/\nu_a)\exp[-(E_{g2} - E_a)/kT] \quad , \quad (6-12)$$

where  $T$  represents  $T_S$  or  $T_{RC}$ . If the substrate was cooled very slowly from the high temperature to room temperature ( $T_{room}$ ), the total density observed from ESR would be expressed as

$$N_S = (c_{sw}N_CN_V/\nu_a)\exp[-(E_{g2} - E_a)/kT_{room}] \quad , \quad (6-13)$$

which means that  $N_S$  should be lower than  $10^{15} \text{ cm}^{-3}$ . However, it is impossible to cool down so slowly. Therefore,  $N_S$  is frozen in at some temperature ( $T_{fr}$ ) which strongly depends on the cooling rate and it is expressed as Eq. (6-13) where  $T_{fr}$  replaces  $T_{room}$ . The actual cooling rate causes the value of  $N_S$  to become of the order of  $10^{15} \text{ cm}^{-3}$ .

In the case of the film deposited at  $200^\circ\text{C}$ ,  $N_I$  in the rapidly-cooled film for  $T_{RC}=200^\circ\text{C}$  was equal to that (about  $10^{16} \text{ cm}^{-3}$ ) in the as-deposited film. The value of  $N_I$  for  $T_{RC}=250^\circ\text{C}$  decreased as low as  $N_I$  (about  $5 \times 10^{15} \text{ cm}^{-3}$ ) in a good quality film. And then  $N_I$  increased with an increase of  $T_{RC}$ . In the case of the good quality films deposited at  $250^\circ\text{C}$  and  $300^\circ\text{C}$ , on the other hand,  $N_I$  (about  $5 \times 10^{15} \text{ cm}^{-3}$ ) did not change in the range of  $T_{RC} \leq 250^\circ\text{C}$ , and then  $N_I$  increased with a further increase of  $T_{RC}$ . The midgap states may equilibrate during the deposition at  $250$ - $300^\circ\text{C}$ , and the midgap states are frozen in at the temperature lower than  $250^\circ\text{C}$  during the real slow cooling because the value of  $N_I$  at  $T_S=300^\circ\text{C}$  was close to that at  $T_S=250^\circ\text{C}$ . From the result of rapid cooling from  $T_{RC}=250^\circ\text{C}$ , the value

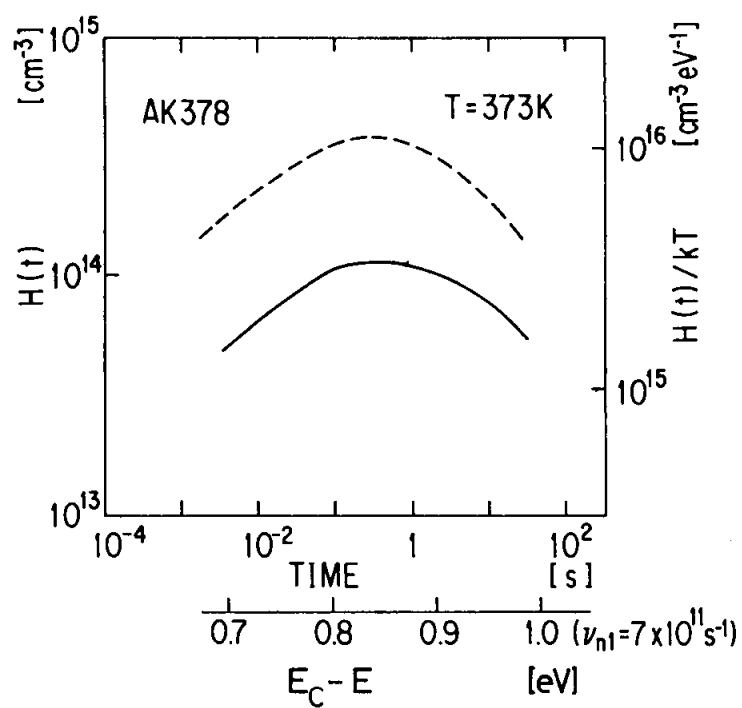


**Fig.6.16.** Change of measured  $H(t)$  by rapid cooling from 300 °C. The solid and broken curves represent  $H(t)$  of as-deposited and rapidly-cooled films, respectively.

## CHAPTER VI CHANGES OF MIDGAP STATES

of  $5 \times 10^{15} \text{ cm}^{-3}$  is considered to correspond to  $N_s$  at equilibrium near  $250^\circ \text{C}$ . Then, when the films are heated up to  $300^\circ \text{C}$ , the midgap states equilibrate at  $300^\circ \text{C}$ , which means that  $N_s$  at equilibrium becomes larger than  $5 \times 10^{15} \text{ cm}^{-3}$ . By the rapid cooling,  $N_s$  becomes close to  $N_s$  at equilibrium near  $300^\circ \text{C}$ , resulting in the increase of  $N_s$ . The deposition condition of  $T_s = 200^\circ \text{C}$ , which is considered not to obey Eq. (6-12), is not good. So, this film has a lot of midgap states even if the substrate is cooled down slowly. When this film is heated to  $250^\circ \text{C}$ , the midgap states equilibrate at  $250^\circ \text{C}$  according to Eq. (6-12). The rapid cooling makes the value of  $N_s$  keep at the condition near  $250^\circ \text{C}$ .

From the transient HMC method, the states increased by rapid cooling from  $300^\circ \text{C}$  were the states having  $\nu_{n1}$ , since  $t_p$  in the rapid cooling film was the same as  $t_p$  in the as-deposited film, as shown in Fig. 6.16. Therefore, the metastable states induced by rapid cooling are assigned to the midgap states in as-deposited films.

Finally, these results obtained by the HMC methods are discussed and compared with other results. Both states produced by the light soaking, which are distinguished by the difference in  $\nu_n$ , must originate from electron-spin centers because the behavior of  $N_I$  by light soaking is quite similar to that obtained from ESR. From the study of as-deposited films, the states with  $\nu_{n1}$  are found to be  $D^0$  of Si, and those states could also be thermally created because they exist in the as-deposited and the rapidly-cooled films. On the other hand, the other states with  $\nu_{n2}$ , which will be noted as  $D_L^0$ , can be created only by light soaking.

Han and Fritzsche,<sup>7)</sup> and Qiu et al.<sup>8)</sup> reported that two kinds of metastable states could be produced by light soaking. The first light-induced reversible states had a small capture-cross section ( $\sigma_{n1}$ ) for electrons, and were detected by a constant photocurrent measurement (CPM). The second states had a large capture-cross section ( $\sigma_{n2}$ ) for electrons, and were detected by an increment ( $\Delta \sigma_p$ ) of conductivity using a small incident light flux with a 2-eV photon energy. The value of  $\sigma_{n1}$

## CHAPTER VI CHANGES OF MIDGAP STATES

was smaller by about one order of magnitude than  $\sigma_{n2}$ , and both states were located in the midgap. The value of  $\Delta\sigma_p$  decreased by the short-time (3-4 h) light soaking at 100 K, while an absorption coefficient ( $\alpha_1$ ) at 1.0 eV obtained from CPM did not change. By the same light soaking at 300 K, however,  $\Delta\sigma_p$  decreased and  $\alpha_1$  increased. The values of  $\Delta\sigma_p$  and  $\alpha_1$  are expressed as

$$\Delta\sigma_p = B_2 / (\sigma_{n1} N_1 + \sigma_{n2} N_2) \quad (6-14)$$

and

$$\alpha_1 = B_3(N_1 + N_2) \quad , \quad (6-15)$$

respectively, and

$$\sigma_{n2} \approx 10 \sigma_{n1} \quad , \quad (6-16)$$

where  $B_2$  and  $B_3$  are constants,  $N_1$  is the density of the first states, and  $N_2$  is the density of the second states. If the value of  $N_2$  were smaller by the order of 10 than the value of  $N_1$ , the increment of  $N_2$  could hardly be detected by the increment of  $\alpha_1$  according to Eq. (6-15), but it could easily be detected by the change of  $\Delta\sigma_p$  according to Eq. (6-14) because of Eq. (6-16). Therefore, these indicate that the density of the first states increases only at high temperature, while the density of the second states increases at any temperature and that the value of  $N_2$  is still smaller than that of  $N_1$  in the short-time light-soaking. In the light of our results, the first states correspond to  $D^0$  just as they concluded, and the second states should correspond to  $D_L^0$  because  $\nu_n$  is proportional to  $\sigma_n$ . Indeed, in the case of deuterated amorphous silicon (a-Si:D), only the midgap states with  $\nu_{n1}$  were reported to increase by light-soaking.<sup>15)</sup> That is why the rate of conductivity decrease in a-Si:D is reported to be smaller than that in a-Si:H. The origin of  $D_L^0$  is still an open question, although Okushi et al.<sup>16)</sup> have insisted a model in which the dangling-bond-like centers are

## CHAPTER VI CHANGES OF MIDGAP STATES

produced by a spatially intimated coupling of pairs between dangling bonds and positively ionized impurities.

### 6-5. Summary

(1) The steady-state and transient HMC methods have been applied to determining densities and profiles of midgap states in undoped  $a\text{-Si}_{1-x}\text{Ge}_x\text{:H}$ , undoped  $a\text{-Si:H}$  and undoped  $a\text{-Si}_{1-x}\text{C}_x\text{:H}$ . The midgap states are correlated with  $D^0$ ; the density in  $a\text{-Si}_{1-x}\text{Ge}_x\text{:H}$  ( $E_0 \leq 1.63$  eV) represents the  $D^0$  density of Ge, and in  $a\text{-Si:H}$  and  $a\text{-Si}_{1-x}\text{C}_x\text{:H}$  ( $E_0 \leq 1.88$  eV) it represents the  $D^0$  density of Si. The density of midgap states increases slowly with the Ge content in the film, while it increases rapidly with the C content. The peak of the midgap-state profile appears clearly in  $a\text{-Si:H}$  and  $a\text{-Si}_{1-x}\text{Ge}_x\text{:H}$ , but it does not appear clearly in  $a\text{-Si}_{1-x}\text{C}_x\text{:H}$ .

(2) Thermal annealing kinetics of metastable gap states in short-time light-soaked  $a\text{-Si:H}$  have been investigated. Monomolecular kinetics are suitable for explaining the experimental data. The thermal activation energy ( $E_a$ ) for annealing decreases monotonously with an increase in  $(E_C - E)$ . This is the first report which elucidates the relation between  $E_a$  and  $(E_C - E)$ .

(3) The midgap states having a small  $\nu_n$  are created both optically and thermally, while the midgap states having a large  $\nu_n$  are created only by light soaking. Both states are located around 0.85 eV below the conduction band edge.